Reflectance spectra recovery from tristimulus values by adaptive estimation with metameric shape correction

Simone Bianco[1,*]

[1] *DISCo - Dipartimento di Informatica, Sistemistica e Comunicazione, Universit degli studi di Milano-Bicocca, Viale Sarca 336, Edificio U14, 20126, Milano, Italy*

[*] *Corresponding author: simone.bianco@disco.unimib.it*

Compiled June 23, 2010

In this work is a local optimization-based method which is able to recover the reflectance spectra with the desired tristimulus values, choosing the metamer with the most similar shape to the reflectances available in the training set, is proposed. Four different datasets of reflectance spectra and three different error metrics have been used in this study. According to all the error metrics considered, the proposed algorithm was able to recover the spectral reflectances with higher accuracy than all the state of the art methods considered.

1. Introduction

The most used representation of colors is with a standard trichromatic color coordinate system. There are cases in which this representation is not enough. This representation, besides being illuminant and observer-dependent, is also affected by metameric issues. The most informative and complete way to describe a color is to give its reflectance spectra, which is defined as the ratio of the reflected light to the incident light. The reflectance spectra can be directly measured using spectrophotometers; unfortunately the most used color acquisition devices capture the color signal by acquiring only three channels. Since the reflectance spectra is essential for many applications, the problem of recovering the reflectance spectra from triplets in a trichromatic color coordinate system has been extensively studied. Dupont in his comparative study [1] considers several optimization methods to recover the spectra reflectances, including the simplex method, the simulated annealing method, the Hawkyard method, genetic algorithms and neural networks. All the methods considered are global methods, which give a global solution. Recent works have improved the spectra recovery accuracy using local methods [2, 3].

The method proposed in this work is a local optimization-based method which is able to recover the reflectance spectra with the desired tristimulus values, choosing the metamer with the most similar shape to the reflectances available in the training set.

The novelty of the paper comes from the introduction of a new optimization function composed by heterogeneous terms: a colorimetric error term, a spectral error term and two shape feasibility terms.

The performance assessment of the proposed method and of the benchmarking algorithms considered has been done on four different spectral dataset in terms of different colorimetric errors, different spectral similarity metrics and spectral residuals plots. The sensitivity analysis of the proposed optimization function with respect to the various terms of which it is composed is also reported.

According to all the error metrics considered, the proposed algorithm was able to recover the spectral reflectances with higher accuracy than all the benchmarking methods considered, which are described in the next section.

2. Reflectance spectra recovery: problem formulation and related works

The CIE XYZ tristimulus values of a surface with spectral reflectance $r(\lambda)$ that is viewed under an illuminant with spectral power distribution $I(\lambda)$ can be determined as

$$\begin{aligned} X &= k \int r(\lambda) I(\lambda) \overline{x}(\lambda) \mathrm{d}\lambda \\ Y &= k \int r(\lambda) I(\lambda) \overline{y}(\lambda) \mathrm{d}\lambda \\ Z &= k \int r(\lambda) I(\lambda) \overline{z}(\lambda) \mathrm{d}\lambda \end{aligned} \tag{1}$$

with

$$k = \frac{100}{\int I(\lambda) \overline{y}(\lambda) \mathrm{d}\lambda} \tag{2}$$

where $\overline{x}(\lambda), \overline{y}(\lambda)$ and $\overline{z}(\lambda)$ are the CIE color matching functions, and the integral is computed over the visible spectrum.

In practice, spectral functions can be represented by their samples, and spectral integrals may be approximated by sums. If spectral functions are evenly sampled at N wavelengths, then Eqs. (1) can be written as

$$\begin{bmatrix} X \\ Y \\ Z \end{bmatrix} = \mathbf{M}\mathbf{r} \tag{3}$$

where $\mathbf{M}$ is a $3 \times N$ matrix with the samples of $I(\lambda)\overline{x}(\lambda), I(\lambda)\overline{y}(\lambda)$ and $I(\lambda)\overline{z}(\lambda)$ stacked row-wise, and $\mathbf{r}$ is a $N \times 1$ spectral reflectance vector made of the samples of $r(\lambda)$.

The problem of recovering the reflectance spectra from tristimulus values is that of estimating $\mathbf{r}$ from the output of Eq. (3).

The most immediate and straightforward solution is to use the pseudo-inverse algorithm [4]:

$$\mathbf{r} = \left(\mathbf{M}^T\mathbf{M}\right)^{-1}\mathbf{M}^T \begin{bmatrix} X \\ Y \\ Z \end{bmatrix} = \mathbf{M}^+ \begin{bmatrix} X \\ Y \\ Z \end{bmatrix} \tag{4}$$

The performance of the pseudo-inverse algorithm in the case of an inadequate number of data points is not too good and could yield atypical spiky estimates of the spectrum, which are due to the inversion of a $N \times N$ bad conditioned matrix.

The most successful approaches for the estimation of the spectral reflectance from the CIE XYZ values are based upon applying dimensionality reduction techniques. The algorithm was originally formulated by Fairman and Brill [5]. This method exploits linear models to represent each reflectance through the weighted sum of a small number k of basis function $\mathbf{v}_i$:

$$\mathbf{r} \approx \overline{\mathbf{v}} + \sum_{i=1}^{k} a_i \mathbf{v}_i \tag{5}$$

where $\overline{\mathbf{v}}$ denotes the mean of the spectral reflectances of the training set, $\mathbf{v}_i$ is the i-th basis vector of the Principal Component Analysis (PCA) and is calculated from the spectral reflectances of the training set after subtracting $\overline{\mathbf{v}}$, and a_i denotes the coefficient of the corresponding PCA basis vector. Since we have only one set of CIE XYZ tristimulus values for each reflectance we want to recover, k in Eq. (5) takes the value of 3. Substituting Eq. (5) into Eq. (3) yields

$$\begin{bmatrix} X \\ Y \\ Z \end{bmatrix} = \mathbf{M}\overline{\mathbf{v}} + \mathbf{M}\left[\mathbf{v}_1\ \mathbf{v}_2\ \mathbf{v}_3\right] \begin{bmatrix} a_1 \\ a_2 \\ a_3 \end{bmatrix} = \mathbf{M}\overline{\mathbf{v}} + \mathbf{M}\mathbf{V} \begin{bmatrix} a_1 \\ a_2 \\ a_3 \end{bmatrix} \tag{6}$$

which can be easily inverted to find the coefficients $a_i,\ i = 1, \ldots, 3$:

$$\begin{bmatrix} a_1 \\ a_2 \\ a_3 \end{bmatrix} = (\mathbf{M}\mathbf{V})^{-1} \left(\begin{bmatrix} X \\ Y \\ Z \end{bmatrix} - \mathbf{M}\overline{\mathbf{v}} \right) \tag{7}$$

The main advantage of this method is that now we have to invert a 3×3 matrix that is better conditioned and produces less spiky estimates of the spectrum. The final estimated spectrum is then obtained substituting the output of Eq. (7) into Eq. (5).

In order to use more PCA basis vectors, Harifi et al. [6] proposed a modified version of the previous method in order to estimate the CIE XYZ values under a second illuminant. This permits to have twice the information and thus to use $k = 6$ PCA basis vectors. The CIE XYZ values under a second illuminant are estimated from the ones under the given illuminant by a 3×11 polynomial transformation matrix. Eq. (7) then becomes

$$\begin{bmatrix} a_1 \\ a_2 \\ a_3 \\ a_4 \\ a_5 \\ a_6 \end{bmatrix} = (\mathbf{M}\mathbf{V})^{-1} \left(\begin{bmatrix} X_{ill1} \\ Y_{ill1} \\ Z_{ill1} \\ X_{ill2} \\ Y_{ill2} \\ Z_{ill2} \end{bmatrix} - \mathbf{M}\overline{\mathbf{v}} \right) \tag{8}$$

where now $\mathbf{V} = [\mathbf{v}_1\ \mathbf{v}_2\ \mathbf{v}_3\ \mathbf{v}_4\ \mathbf{v}_5\ \mathbf{v}_6]$.

In order to improve the reconstruction accuracy of the PCA method, Zhang and Xu [2] proposed a local PCA method. They used different sets of principal components, one for each of the tonal subgroups they considered. They defined 11 tonal subgroups including 10 different hues and a near gray region. If the chroma of each reflectance was less than 15, it was heuristically defined as belonging to the near gray subgroup. If the chroma was greater than 15 it was assigned to one of the 10 hue subgroups into which the spectral space was divided according to 10 separate hue angles in the Munsell space.

Mansouri et al. [3] proposed an adaptive PCA algorithm for reflectance estimation. The algorithm first computes a global PCA basis for all the training set and estimates the reflectance using Eq. (7) and Eq. (5). Then it measures the likelihood between the estimated reflectance and each element of the training set. A new training set is build by keeping only those elements whose similarity falls in the range $[95\%, 100\%]$. Then a new PCA analysis is performed from this new set to derive a new basis with which the final estimation is done. The likelihood is calculated using the non centered correlation coefficient, commonly known as Goodness of Fit Coefficient (GFC) [7]:

$$GFC = \frac{\sum_{j=1}^{N} r_j \hat{r}_j}{\left[\sum_{j=1}^{N} (r_j)^2\right]^{1/2} \left[\sum_{j=1}^{N} (\hat{r_j})^2\right]^{1/2}} \tag{9}$$

where r_j and $\hat{r_j}$ are the j-th samples of the original and reconstructed spectrum respectively.

A different approach that does not use any dimensional reduction technique is the Hawkyard method [8]. It is an iterative method, and its principle states that the reflectance spectrum is the weighted sum of the primary functions. The primary functions are defined as the rows $[\mathbf{m}_1\ \mathbf{m}_2\ \mathbf{m}_3]^T$ of the matrix $\mathbf{M}$ of Eq. (3). Given the tristimulus value X, Y, Z of the reflectance we want to recover, the initial estimate is computed as

$$\mathbf{r}_{est} = \frac{X_o\mathbf{m}_1 + Y_o\mathbf{m}_2 + Z_o\mathbf{m}_3}{\mathbf{m}_1 + \mathbf{m}_2 + \mathbf{m}_3} \tag{10}$$

where $[X_o\ Y_o\ Z_o] = [X\ Y\ Z]$. From this reflectance curve the corresponding tristimulus values X', Y', Z' are cal-

culated using Eq. (3). Then the differences

$$\begin{aligned}\Delta X &= X' - X \\ \Delta Y &= Y' - Y \\ \Delta Z &= Z' - Z\end{aligned} \tag{11}$$

are calculated and X_o, Y_o, Z_o in Eq. (10) are replaced as

$$\begin{aligned}X_o &= X_o - \Delta X \\ Y_o &= Y_o - \Delta Y \\ Z_o &= Z_o - \Delta Z\end{aligned} \tag{12}$$

The process is repeated until the required accuracy or the maximum number of iterations has been reached.

All the algorithms described have the problem that the recovered reflectance spectra can be unfeasible: in fact the recovered reflectance can present lobes outside the range $[0\%, 100\%]$, or can present atypical spikes due to the recontruction method or to the clipping of the recovered reflectance in the admissible range. To address these problems Zuffi et al. [9] proposed an algorithm to obtain feasible reflectance spectra. The algorithm starts with estimating the recovered reflectance $\mathbf{r}_0$ through Eq. (7) and Eq. (5) and then decomposing it as

$$\mathbf{r}_0 = \mathbf{r}_{0,f} + \mathbf{r}_{0,+} + \mathbf{r}_{0,-} \tag{13}$$

where $\mathbf{r}_{0,f}$,$\mathbf{r}_{0,+}$,$\mathbf{r}_{0,-}$ are the parts of spectrum inside, above and under the admissible range, respectively. The tristimulus values of $\mathbf{r}_{0,+}$ and $-\mathbf{r}_{0,-}$ are computed and given as input to Eq. (7) and Eq. (5) to obtain $\tilde{\mathbf{r}}_{0,+}$ and $\tilde{\mathbf{r}}_{0,-}$. A new reflectance is defined as

$$\mathbf{r}_1 = \mathbf{r}_{0,f} + \tilde{\mathbf{r}}_{0,+} + \tilde{\mathbf{r}}_{0,-} \tag{14}$$

This new reflectance is decomposed into $\mathbf{r}_{1,f}$,$\mathbf{r}_{1,+}$ and $\mathbf{r}_{1,-}$. A smoothing procedure can be run on $\mathbf{r}_{1,+}$ and $\mathbf{r}_{1,-}$ which are then given as input to Eq. (7) and Eq. (5). All the operation described are looped until a the required accuracy or the maximum number of iteration has been reached.

3. The proposed algorithm

The proposed algorithm starts using a dimensionality reduction technique on the measured training reflectances $\mathbf{r}$ to have a linear base $\mathbf{V}_0$ for them by first subtracting the average value $\overline{\mathbf{v}}_0$ of the spectral reflectances of the training set.

An initial estimate $\mathbf{r}_0$ of the reconstructed spectra is then obtained using Eq. (7).

The spectral residuals $\mathbf{b}$ between the reconstructed spectra $\mathbf{r}_0$ and the measured spectra $\mathbf{r}$ are then computed, i.e. $\mathbf{b} = \mathbf{r} - \mathbf{r}_0$. The average spectral residual $\overline{\mathbf{b}}$ is computed and subtracted, and a dimensionality reduction technique is employed to extract a linear basis $\mathbf{B}$ for $\mathbf{b} - \overline{\mathbf{b}}$.

The likelihood between the initial estimate $\mathbf{r}_0$ of the spectra and each element of the training set is then measured using the GFC in Eq.(9). The samples with a normalized likelihood in the range $[p, 1]$ are retained and a dimensionality reduction technique is employed to extract a linear basis $\mathbf{V}_1$ for them by first subtracting their average reflectance value $\overline{\mathbf{v}}_1$.

An optimization routine is then run to estimate the coefficients $[\hat{a}_1, \ldots, \hat{a}_6]$ to give to the basis $\mathbf{V}_1$ and $\mathbf{B}$ in order to give the final reflectance estimation $\hat{\mathbf{r}}$. The optimization function used is composed of four different terms: a colorimetric error term, two shape feasibility terms, and a spectral error term.

Before introducing the optimization function, we have to first define the terms of which it is composed. Let us define $\Delta E_{94}(\mathbf{r}, \hat{\mathbf{r}})$ as the ΔE_{94} colorimetric error under the CIE D65 illuminant between the computed *Lab* values of the estimated $\hat{\mathbf{r}}$ and the measured $\mathbf{r}$; as colorimetric error, the ΔE_{94} is chosen as it is a refinement of the ΔE_{76} error, it is computationally simpler than successive error metrics ΔE_{2000} and ΔE_{CMC}, and permits to leave the ΔE_{2000} and ΔE_{CMC} as test metrics. For the shape feasibility, let us define $u_-(\hat{\mathbf{r}})$ as the sum of the values assumed by the recovered reflectance below the normalized admissible range $[0, 1]$, i.e.

$$u_-(\hat{\mathbf{r}}) = \sum_{j=1}^{N} \hat{r}_j : \hat{r}_j < 0 \; ; \tag{15}$$

let us define $u_+(\hat{\mathbf{r}})$ as the sum of the values assumed by the recovered reflectance above the admissible range $[0, 1]$, i.e.

$$u_+(\hat{\mathbf{r}}) = \sum_{j=1}^{N} \hat{r}_j : \hat{r}_j > 1 \; ; \tag{16}$$

for the spectral error, let us define GFC_{max} as the maximum GFC between the recovered $\hat{\mathbf{r}}$ and all the reflectances in the training set.

Then the recovered reflectance $\hat{\mathbf{r}}$ can be found by

$$\hat{\mathbf{r}} = \overline{\mathbf{v}}_1 + \mathbf{V}_1 \begin{bmatrix} \hat{a}_1 \\ \hat{a}_2 \\ \hat{a}_3 \end{bmatrix} + \overline{\mathbf{b}} + \mathbf{B} \begin{bmatrix} \hat{a}_4 \\ \hat{a}_5 \\ \hat{a}_6 \end{bmatrix} \tag{17}$$

where

$$\begin{bmatrix} \hat{a}_1 \\ \vdots \\ \hat{a}_6 \end{bmatrix} = \min_{\mathbf{x} \in \mathbb{R}^6} \quad \alpha \cdot \Delta E_{94}(\mathbf{r}, \hat{\mathbf{r}}) + \beta \cdot u_-(\hat{\mathbf{r}}) + \\ + \gamma \cdot u_+(\hat{\mathbf{r}}) + \delta \cdot (1 - GFC_{max}) \tag{18}$$

are the values found by optimization. Equation (18) is then the optimization function adopted. It is possible to notice that it is composed by four different terms: the first one is a colorimetric error, which is used to find the most colorimetrically similar solution. The second and third one are shape feasibility terms: they are used to find a solution which has values in the admissible range [0,1]. The fourth term is a spectral error, which is used to find the solution which is the most spectrally similar to the reflectances in the training set. The use of the colorimetric error in the optimization function is a common

choice for optimization based algorithms for the recovery the spectra reflectances [1]. The use of the shape feasibility terms has been inspired by the work of Zuffi et al. [9], although here they are used in a different way. Finally, the use of the spectral error term, proposed by Mansouri et al. [3] as a criterion to choose a subset of the training set on which to compute the refined PCA basis, it is used here to produce the solution which is the most spectrally similar to the reflectances in the training set, and thus the most spectrally likely.

The algorithm is reported in pseudo-code in Table 1.

The dimensionality reduction technique employed for this algorithm is the Independent Component Analysis (ICA) [10]. ICA was developed to find statistically independent components in the general case where the data is non-gaussian, which makes it different from other factor analysis techniques where the data is modeled as linear mixtures of some underlying factors [11].

The weights in Eq.(18) are heuristically chosen as $[\alpha, \beta, \gamma, \delta] = [1, 100, 100, 1]$ in order to be sure that the optimization algorithm finds first a feasible spectra and then optimizes simultaneously the colorimetric and the spectral errors. The weights β, γ are chosen two orders of magnitude higher than α, δ to prevent unfeasible solutions. Obviously a different choice for the weights could be made, and different terms could be used in the optimization function. As a further analysis, the sensitivity of the algorithm with respect to the weights $[\alpha, \beta, \gamma, \delta]$ is reported in the appendix.

The optimization algorithm used is the Pattern Search [12] which is a direct search method for nonlinear optimization that does not require any explicit estimate of derivatives. The general form of a Pattern Search Method can be described in the following way. At each step k, we have the current iterate $\mathbf{x}_k$, a set D_k of search directions, and a step-length parameter Δ_k. Usually the set D_k is the same for all iterations. For each direction $\mathbf{d}_k \in D_k$, we set $\mathbf{x}^+ = \mathbf{x}_k + \Delta_k \mathbf{d}_k$ (the "pattern") and we examine $f(\mathbf{x}^+)$ where f is the function to be minimized. If $\exists \mathbf{d}_k \in D_k : f(\mathbf{x}^+) < f(\mathbf{x}_k)$, we set $\mathbf{x}_{k+1} = \mathbf{x}^+$ and $\Delta_{k+1} = \alpha_k \Delta_k$ with $\alpha_k > 1$; otherwise, we set $\mathbf{x}_{k+1} = \mathbf{x}_k$ and $\Delta_{k+1} = \beta_k \Delta_k$ with $\beta_k < 1$. The algorithm stops when step Δ_k is smaller than a fixed threshold, or when the maximum number of iterations has been reached. In this work we have chosen $\alpha_k = 2$, $\beta_k = 0.5$, $D_k = \{\pm\mathbf{e}_1, \pm\mathbf{e}_2, \pm\mathbf{e}_3, \pm\mathbf{e}_4, \pm\mathbf{e}_5, \pm\mathbf{e}_6\}$ (i.e. the six versors of the Cartesian coordinate system of the Euclidean space $\mathbb{R}^6$ taken with both positive and negative direction), and $\Delta_0 = 0.1$.

Finally, the likelihood range to select the reflectances used to extract the local basis $\mathbf{V}_1$ is set $[0.95, 1]$, i.e. $p = 0.95$.

4. Experimental setup

The experimental data includes five different data sets: one was used as a training set for all the methods of Sections 2 and 3, the other four were used as test sets.

Table 1. Pseudo-code of the proposed algorithm

```
Begin
 Derive a basis V0 for the whole training set
 Estimate the recovered spectra
 Calculate the spectral residuals between the
 recovered and the training set spectra
 Derive a basis B for the spectral residuals
 Use the basis V0 to give an initial estimate of
 the recovered spectra using Eq.(5)
 for each initial estimate of the recovered spectra
 Do
  Calculate the GFC with the spectra in the training set
  Derive a basis V1 for the spectra with GFC ∈ [p,1]
  Minimize Eq.(18)
  Compute the final recovered spectra using Eq.(17)
 End
End
```

The training set is composed of the odd samples of the Munsell Atlas. The even samples of the Munsell Atlas, the 170 samples of the Vhrel dataset [13], the 24 samples of the GretagMacbeth Color Checker CC, the central 172 samples of the GretagMacBeth Color Checker DC (except the 8 glossy samples) were used as test sets. All the data were sampled from 400nm to 700nm in 10nm steps.

Five different error metrics are used to assess the performance of the considered algorithms: the ΔE_{94} colorimetric error under the training CIE D65 illuminant and under the CIE A and CIE F2 illuminants; the peak signal to noise ratio (PSNR), which for two n-dimensional reflectances $\mathbf{r}$ and $\hat{\mathbf{r}}$ is defined as

$$\mathrm{PSNR}(\mathbf{r}, \hat{\mathbf{r}}) = 20 \cdot \log_{10} \frac{1}{\sqrt{\frac{1}{n} \sum_{i=1}^{n} (\mathbf{r}_i - \hat{\mathbf{r}}_i)^2}}, \qquad (19)$$

and the goodness of fit coefficient (GFC, see Eq.(9)).

5. Experimental results

The experimental results are reported in Table 2. Three different statistics are reported for the ΔE_{94}: the average value, the 95% percentile and the standard deviation. Following [14] the PSNR values have been subdivided into three intervals: PSNR$<$ 34dB, 34dB$\leq$PSNR$<$ 40dB and PSNR$\geq$ 40dB which correspond to a poor, accurate and good spectral estimation respectively. Following [14] the GFC values have been subdivided into four intervals: GFC$<$ 0.995, 0.995 $\leq$GFC$<$ 0.999, 0.999 $\leq$GFC$<$ 0.9999 and GFC$\geq$ 0.9999 which correspond to a poor, accurate, good and excellent spectral estimation respectively. For each of the considerd intervals the percentage of spectra within it is reported. Although the GFC has already been used as spectral similarity term in the optimization function reported in Eq. (18) it is here used differently: in the optimization function it was used to find the most likely solution, i.e. the most spectrally similar solution to the spectra reflectances in the training

set; here it is used as a similarity measure between the reconstructed and measured spectra.

It can be seen from Table 2 that only two out of the seven benchmarking methods considered were able to always recover a spectra with almost the same tristimulus values under the CIE D65 training illuminant: they are the HAW [8] and the ZSS [9]. The colorimetric errors under the CIE A and F2 illuminants show that none of them was able to perfectly reconstruct the spectra. Among the benchmarking algorithms considered, the ones with the highest overall performances are the adaPCA [3] and the PCAmuBa [2]. Both of them were unable to give a perfect metameric solution under the CIE D65 training illuminant, but were able to obtain lower colorimetric errors under the CIE A and F2 test illuminants with respect to the HAW and ZSS algorithms. Better results are obtained also for the spectral similarity measures PSNR and GFC.

It is possible to notice that the proposed method is able to always recover a spectra with almost the same tristimulus values under the CIE D65 training illuminant, almost halving the colorimetric errors under the CIE A and F2 testing illuminant with respect to the HAW and ZSS methods. Furthermore the proposed method is also able to lower the colorimetric errors obtained by the most performing benchmarking algorithms, i.e. adaPCA and PCAmuBa. For what concerns the PSNR and GFC error metrics, it can be noticed that the proposed method reaches the highest good/excellent percentage of reconstruction with respect to all the benchmarking algorithms considered.

In Table 3 the average ΔE_{2000} and $\Delta E_{CMC2:1}$ colorimetric errors between the measured and reconstructed spectra under the CIE D65, A and F2 illuminants are reported. It is possible to notice that even using different colorimetric errors, the ranking of the considered methods remains unchanged with respect to Table 2.

In order to objectively evaluate the performance of the methods considered, and to assess if they are statistically significant, the Wilcoxon sign test (WST) [15] is used. The WST is a statistical test able to compare the whole error distributions of two methods, without making any assumptions about the underlying error distribution. Making all the pairwise comparisons among the ΔE_{94} error distributions obtained by the considered algorithms on each different dataset, it is possible to generate a score representative of the number of times that each algorithm has been considered better or equivalent to the others. All the pairwise comparison are done with a significance level $\alpha = 0.05$. The scores obtained for the ΔE_{94} error distributions under the CIE D64, A and F2 illuminants are reported in Table 4. The best score for each column is reported in bold. It can be noticed that for all the dataset-illuminant combinations considered, the proposed algorithm always gives the best spectral reconstruction. The scores obtained for the ΔE_{2000} and $\Delta E_{CMC2:1}$ error distributions are not reported as being identical to the ones reported in Table 4.

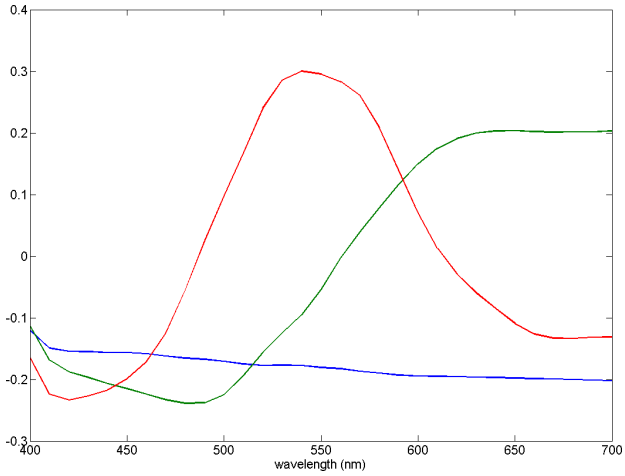

Fig. 1. (Color online) The ICA basis $\mathbf{V}_0$ obtained from the training set

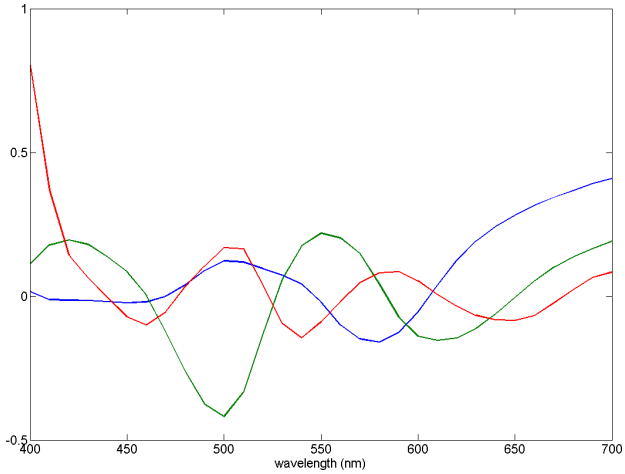

Fig. 2. (Color online) The ICA basis $\mathbf{B}$ obtained from the spectral residuals

The initial ICA basis $\mathbf{V}_0$ obtained for the proposed algorithm on the training set is reported in Figure 1, while the ICA basis $\mathbf{B}$ of the spectral residuals is reported in Figure 2. The computation of the tristimulus values shows that the basis $\mathbf{V}_0$ and then $\mathbf{V}_1$ are the ones that are used by the proposed algorithm to try to reconstruct a spectra with the desired tristimulus values. The basis $\mathbf{B}$, having tristimulus values with a magnitude in the order of 10^{-15} is used by the proposed algorithm to correct the shape of the reconstructed spectra adding a linear combination of metameric blacks, thus identifying the metameric solution which minimizes Eq. (18).

In Figures 3-7 the average spectral residuals between measured and reconstructed spectra are reported as a function of wavelength. In each figure all the considered methods are compared on a different dataset: the half Munsell dataset used as training set (Fig. 3), the other half Munsell dataset (Fig. 4), the Vhrel dataset (Fig. 5), the MCC dataset (Fig. 6) and the MDC dataset (Fig. 7), which are all used as test sets. From the analysis

Table 2. Algorithms performance on all the datasets considered: average, 95% percentile and standard deviation of the ΔE_{94} colorimetric error under the CIE D65, A and F2 illuminants; percentages of reconstructed spectra with a poor, accurate and good reconstruction judged by PSNR; percentages of reconstructed spectra with a poor, accurate, good and excellent reconstruction judged by GFC.

		ΔE_{94} under ill. D65			ΔE_{94} under ill. A			ΔE_{94} under ill. F2			PSNR			GFC			
Method	Dataset	Mean	95%	std	Mean	95%	std	Mean	95%	std	poor	accurate	good	poor	accurate	good	excellent
PINV [4]	MUNStr	0.0042	0.0000	0.0848	0.7843	2.3871	0.8457	0.7625	2.2980	0.8460	44.2520%	33.8583%	21.8898%	20.0000%	58.1102%	21.8898%	0.0000%
	MUNSte	0.0036	0.0000	0.0523	0.8457	3.0222	0.9255	0.7718	2.3908	0.8035	44.4795%	33.4385%	22.0820%	21.9243%	56.9401%	21.1356%	0.0000%
	VHRELte	0.0940	0.0432	0.5234	1.1286	2.5267	1.0055	1.0399	2.5929	1.3368	69.4118%	17.0588%	13.5294%	71.7647%	17.0588%	11.1765%	0.0000%
	MCCte	0.0830	0.5974	0.4065	1.3037	4.1796	1.3174	1.4769	5.2472	1.7519	75.0000%	12.5000%	12.5000%	45.8333%	41.6667%	12.5000%	0.0000%
	MDCte	0.0428	0.0917	0.2745	1.1370	3.7136	1.1817	1.2244	3.7235	1.4539	62.2093%	22.0930%	15.6977%	37.7907%	44.7674%	17.4419%	0.0000%
PINV-PCA[5]	MUNStr	0.0051	0.0000	0.0786	0.8097	2.7608	0.9418	0.7699	2.3452	0.8257	48.3465%	36.8504%	14.8031%	28.0315%	58.2677%	13.0709%	0.6299%
	MUNSte	0.0038	0.0000	0.0440	0.8609	3.4918	1.0436	0.7739	2.3586	0.7929	47.4763%	36.4353%	16.0883%	26.4984%	60.0946%	12.6183%	0.7886%
	VHRELte	0.0920	0.3329	0.4898	1.1299	2.5514	0.9649	1.0437	2.4659	1.2800	71.1765%	15.8824%	12.9412%	74.7059%	17.6471%	7.6471%	0.0000%
	MCCte	0.0750	0.5401	0.3675	1.2713	4.0579	1.3615	1.4458	4.9712	1.6787	66.6667%	12.5000%	20.8333%	50.0000%	37.5000%	8.3333%	4.1667%
	MDCte	0.0513	0.1544	0.2688	1.1707	3.8038	1.2388	1.2456	3.5843	1.4073	63.9535%	25.5814%	10.4651%	41.2791%	40.6977%	18.0233%	0.0000%
HAW [8]	MUNStr	0.0000	0.0000	0.0000	0.7996	2.7808	0.8978	0.9844	3.6244	1.1516	55.2756%	22.6772%	22.0472%	29.9213%	52.1260%	17.9528%	0.0000%
	MUNSte	0.0000	0.0000	0.0000	0.8645	3.0196	0.9949	0.9969	3.7305	1.1228	56.6246%	20.8202%	22.5552%	31.8612%	49.8423%	18.2965%	0.0000%
	VHRELte	0.0000	0.0000	0.0000	1.2896	2.9000	0.9396	1.1256	3.1554	1.0787	74.1176%	15.2941%	10.5882%	76.4706%	19.4118%	4.1176%	0.0000%
	MCCte	0.0000	0.0000	0.0000	1.0593	3.1735	1.1359	1.4547	5.9282	1.9238	62.5000%	20.8333%	16.6667%	58.3333%	20.8333%	20.8333%	0.0000%
	MDCte	0.0000	0.0000	0.0000	1.3299	3.6502	1.2720	1.4741	5.7267	1.6407	77.3256%	11.6279%	11.0465%	51.7442%	42.4419%	4.0698%	1.7442%
adaPCA [3]	MUNStr	0.0000	0.0000	0.0000	0.4642	1.1604	0.4309	0.4570	1.1321	0.3426	28.0315%	37.7953%	34.1732%	9.7638%	51.8110%	37.4803%	0.9449%
	MUNSte	0.0000	0.0000	0.0000	0.5164	1.4516	0.4932	0.4722	1.1692	0.3762	27.7603%	38.8013%	33.4385%	11.6719%	51.5773%	35.8044%	0.9464%
	VHRELte	0.0078	0.0000	0.0773	0.9492	2.2537	0.7310	0.7765	1.9004	0.6225	67.6471%	17.0588%	15.2941%	70.0000%	19.4118%	10.5882%	0.0000%
	MCCte	0.0000	0.0000	0.0000	0.5218	1.9816	0.5884	0.5576	1.8724	0.5655	37.5000%	37.5000%	25.0000%	16.6667%	37.5000%	45.8333%	0.0000%
	MDCte	0.0018	0.0000	0.0242	0.5719	1.7880	0.5890	0.5645	1.5703	0.4561	43.6047%	33.7209%	22.6744%	16.2791%	51.1628%	31.9767%	0.5814%
PCAemRe [6]	MUNStr	0.0032	0.0000	0.0234	0.6730	2.0324	0.7731	0.7071	1.8671	0.5755	50.7087%	32.4409%	16.8504%	39.3701%	40.7874%	19.5276%	0.3150%
	MUNSte	0.0027	0.0000	0.0193	0.7139	2.5211	0.8421	0.7106	1.7824	0.5479	49.5268%	33.7539%	16.7192%	39.5899%	41.6404%	18.1388%	0.6309%
	VHRELte	0.0661	0.2741	0.3463	1.3007	2.7657	0.9474	1.0788	2.7816	0.8968	70.5882%	15.2941%	14.1176%	78.8235%	17.6471%	3.5294%	0.0000%
	MCCte	0.0361	0.2516	0.0830	1.3640	5.4708	1.7111	1.3008	4.4822	1.2857	66.6667%	16.6667%	16.6667%	66.6667%	20.8333%	8.3333%	4.1667%
	MDCte	0.0272	0.1867	0.1131	0.8984	2.8645	0.8924	0.9995	2.6132	0.8467	71.5116%	15.1163%	13.3721%	58.7209%	30.8140%	9.3023%	1.1628%
PCAmuBa [2]	MUNStr	0.0000	0.0000	0.0000	0.3989	1.2129	0.4563	0.3899	1.0863	0.3488	18.5827%	40.0000%	41.4173%	12.4409%	40.0000%	44.0945%	3.4646%
	MUNSte	0.0005	0.0000	0.0119	0.4501	1.6673	0.5543	0.4106	1.2480	0.3913	21.6088%	35.8044%	42.5868%	13.8801%	39.5899%	43.3754%	3.1546%
	VHRELte	0.0028	0.0000	0.0370	1.2769	2.8849	0.8846	1.0444	2.5242	0.7793	74.1176%	14.7059%	11.1765%	74.1176%	21.7647%	4.1176%	0.0000%
	MCCte	0.0000	0.0000	0.0000	0.7286	2.2277	0.7233	0.6732	2.6753	0.7423	58.3333%	20.8333%	20.8333%	29.1667%	41.6667%	25.0000%	4.1667%
	MDCte	0.0000	0.0000	0.0001	0.6103	2.4397	0.6835	0.6077	1.7330	0.5487	48.2558%	27.9070%	23.8372%	20.9302%	42.4419%	36.6279%	0.0000%
ZSS [9]	MUNStr	0.0000	0.0000	0.0000	0.8285	2.6205	0.8743	0.7638	2.1633	0.7533	49.4488%	30.0787%	20.4724%	23.3071%	56.6929%	20.0000%	0.0000%
	MUNSte	0.0000	0.0000	0.0000	0.8867	3.2234	0.9655	0.7729	2.1966	0.7288	48.5804%	29.9685%	21.4511%	24.6057%	56.6246%	18.4543%	0.3155%
	VHRELte	0.0000	0.0000	0.0000	1.0188	2.3545	0.8136	0.8967	2.2590	0.8356	68.8235%	17.0588%	14.1176%	71.1765%	18.2353%	10.5882%	0.0000%
	MCCte	0.0000	0.0000	0.0000	1.2886	3.6157	1.2405	1.3732	4.1437	1.3500	75.0000%	12.5000%	12.5000%	45.8333%	41.6667%	12.5000%	0.0000%
	MDCte	0.0000	0.0000	0.0000	1.1577	3.5928	1.1852	1.1663	3.3409	1.1905	67.4419%	19.1860%	13.3721%	39.5349%	42.4419%	18.0233%	0.0000%
Proposed	MUNStr	0.0000	0.0000	0.0000	0.3299	1.3016	0.4944	0.3710	1.1639	0.3762	18.2677%	24.0945%	57.6378%	10.8661%	33.7008%	40.1575%	15.2756%
	MUNSte	0.0000	0.0000	0.0000	0.3769	1.6527	0.5587	0.3881	1.2903	0.4076	15.4574%	27.2871%	57.2555%	11.5142%	35.4890%	38.0126%	14.9842%
	VHRELte	0.0000	0.0000	0.0000	0.8304	2.2835	0.7957	0.7264	1.8522	0.5404	58.2353%	22.9412%	18.8235%	60.0000%	20.0000%	20.0000%	0.0000%
	MCCte	0.0000	0.0000	0.0000	0.2892	1.6748	0.4690	0.4535	2.0849	0.6328	20.8333%	20.8333%	58.3333%	12.5000%	20.8333%	50.0000%	16.6667%
	MDCte	0.0000	0.0000	0.0000	0.3782	1.9669	0.6606	0.4540	1.4844	0.4889	25.0000%	23.8372%	51.1628%	15.1163%	22.6744%	45.3488%	16.8605%

of Figures 3-7 it is possible to notice how the proposed methods tends to have lower and flatter spectral residual plots.

6. Conclusions

In this work is a local optimization-based method which is able to recover the reflectance spectra with the desired tristimulus values, choosing the metamer with the most similar shape to the reflectances available in the training set, is proposed. The reflectance spectra of the Munsell Atlas, the Vhrel dataset, the GretagMacBeth ColorChecker CC and GretagMacBeth ColorChecker DC were used as samples in this study. Different error metrics have been considered to assess the performance of the proposed methods: the ΔE_{94} colorimetric error under three different illuminants (CIE D65, A and F2), the ΔE_{2000} colorimetric error, $\Delta E_{CMC2:1}$ colorimetric error, the peak signal-to-noise ratio (PSNR) and the goodness-of-fit coefficient (GFC). According to all the error metrics considered, the proposed algorithm was able to recover the spectral reflectances with higher accuracy than

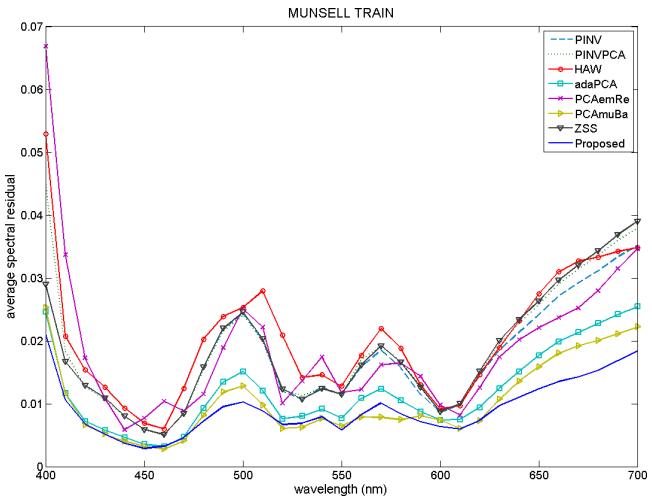

Fig. 3. (Color online) Average spectral residuals between reconstructed and measured spectra on the Munsell training set

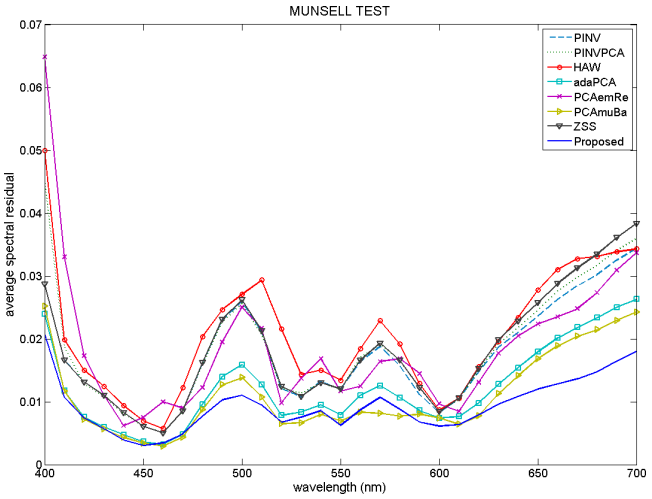

Fig. 4. (Color online) Average spectral residuals between reconstructed and measured spectra on the Munsell test set

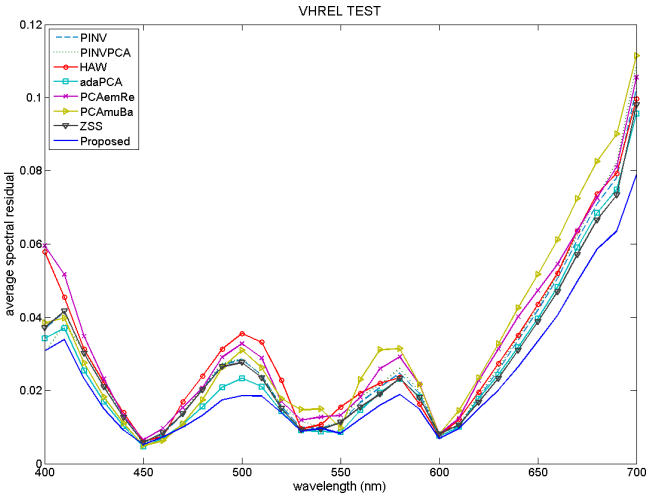

Fig. 5. (Color online) Average spectral residuals between reconstructed and measured spectra on the Vhrel test set

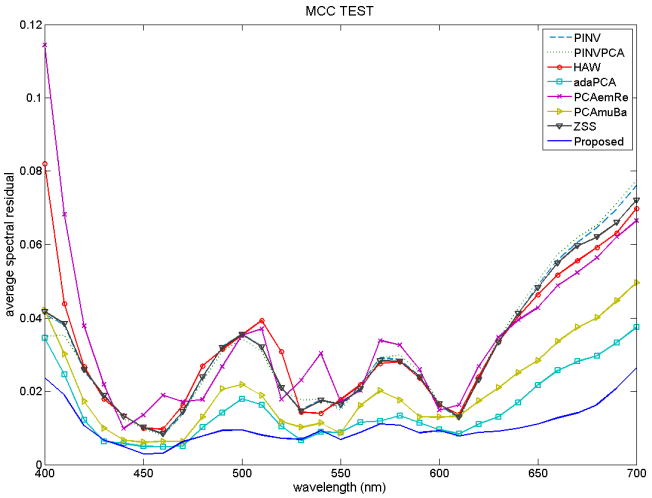

Fig. 6. (Color online) Average spectral residuals between reconstructed and measured spectra on the Macbeth Color Checker CC test set

Table 3. Algorithms performance on all the datasets considered: average ΔE_{2000} and $\Delta E_{CMC2:1}$ errors under D65, A and F2 illuminants

Method	Dataset	ΔE_{2000} D65	A	F2	$\Delta E_{CMC2:1}$ D65	A	F2
PINV [4]	MUNStr	0.0042	0.9079	0.7812	0.0046	1.0869	0.8074
	MUNSte	0.0035	0.9840	0.7964	0.0038	1.1630	0.8165
	VHRELte	0.0949	1.3619	1.0366	0.1090	1.7741	0.9908
	MCCte	0.0840	1.5216	1.4794	0.0904	1.8327	1.4885
	MDCte	0.0429	1.2897	1.2418	0.0462	1.5269	1.2485
PINV-PCA[5]	MUNStr	0.0050	0.9289	0.7794	0.0055	1.0928	0.8021
	MUNSte	0.0038	0.9921	0.7900	0.0042	1.1562	0.8077
	VHRELte	0.0923	1.3656	1.0314	0.1066	1.7888	0.9785
	MCCte	0.0756	1.4631	1.4412	0.0815	1.7590	1.4429
	MDCte	0.0507	1.3141	1.2526	0.0557	1.5470	1.2556
HAW [8]	MUNStr	0.0000	0.9416	1.0066	0.0000	1.1301	1.1330
	MUNSte	0.0000	1.0209	1.0239	0.0000	1.2089	1.1419
	VHRELte	0.0000	1.5671	1.1125	0.0000	2.0318	1.1144
	MCCte	0.0000	1.2435	1.4628	0.0000	1.5516	1.4825
	MDCte	0.0000	1.5560	1.4970	0.0000	1.8372	1.5819
adaPCA [3]	MUNStr	0.0000	0.5603	0.4747	0.0000	0.6721	0.4905
	MUNSte	0.0000	0.6297	0.4921	0.0000	0.7347	0.5022
	VHRELte	0.0074	1.1619	0.7609	0.0087	1.5146	0.6827
	MCCte	0.0000	0.6445	0.5608	0.0000	0.7934	0.5791
	MDCte	0.0018	0.6830	0.5777	0.0020	0.7780	0.5935
PCAemRe [6]	MUNStr	0.0032	0.7832	0.7315	0.0039	0.9446	0.7630
	MUNSte	0.0027	0.8309	0.7341	0.0034	0.9889	0.7648
	VHRELte	0.0681	1.5940	1.0528	0.0835	2.1094	1.0079
	MCCte	0.0355	1.5688	1.2551	0.0415	1.8940	1.2932
	MDCte	0.0270	1.0369	1.0170	0.0315	1.1895	1.0493
PCAmuBa [2]	MUNStr	0.0000	0.4805	0.4114	0.0000	0.5656	0.4315
	MUNSte	0.0005	0.5473	0.4341	0.0006	0.6272	0.4466
	VHRELte	0.0025	1.5628	1.0112	0.0029	2.0598	0.9189
	MCCte	0.0000	0.8983	0.6699	0.0000	1.0868	0.6670
	MDCte	0.0000	0.7239	0.6278	0.0000	0.8278	0.6436
ZSS [9]	MUNStr	0.0000	0.9547	0.7763	0.0000	1.1416	0.7924
	MUNSte	0.0000	1.0264	0.7915	0.0000	1.2142	0.8022
	VHRELte	0.0000	1.2261	0.8907	0.0000	1.6023	0.8360
	MCCte	0.0000	1.4855	1.3606	0.0000	1.7823	1.3557
	MDCte	0.0000	1.2944	1.1735	0.0000	1.5244	1.1730
Proposed	MUNStr	0.0000	0.4014	0.3891	0.0000	0.4810	0.4142
	MUNSte	0.0000	0.4644	0.4098	0.0000	0.5382	0.4299
	VHRELte	0.0000	1.0096	0.7278	0.0000	1.2754	0.6767
	MCCte	0.0000	0.3471	0.4645	0.0000	0.4196	0.5141
	MDCte	0.0000	0.4527	0.4733	0.0000	0.5051	0.5017

Table 4. The Wilcoxon sign test scores, evaluated on the ΔE_{94} error distributions, obtained by the algorithms considered. They are subdivided for each dataset and illuminant considered. The best score for each dataset-illuminant combination is reported in bold. The score is representative of the number of algorithms respect to which the considered algorithm results statistically better or equivalent.

Method	Scores														
	MUNtr			MUNte			VHRELte			MCCte			MDCte		
	D65	A	F2	D65	A	F2	D65	A	F2	D65	A	F2	D65	A	F2
PINV	1	0	2	1	0	1	1	3	3	0	0	0	1	0	0
PINV-PCA	2	0	2	2	0	1	2	3	4	1	0	0	0	0	0
HAW	3	3	0	**3**	3	0	2	0	0	**3**	0	0	3	0	0
adaPCA	**6**	5	5	**3**	4	5	2	3	6	**3**	6	6	**6**	6	5
PCAemRe	0	4	0	0	4	1	0	0	0	2	0	0	1	4	0
PCAmuBa	3	6	6	**3**	6	6	**6**	0	0	**3**	0	0	3	6	5
ZSS	3	0	2	**3**	0	1	2	3	4	**3**	0	0	3	0	0
Proposed	**6**	**7**	**7**	**3**	**7**	**7**	**6**	**7**	**7**	**3**	**7**	**7**	**6**	**7**	**7**

all the state of the art methods considered.

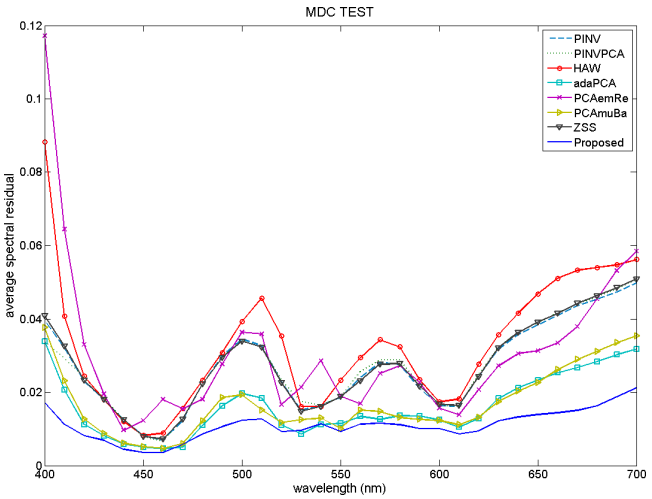

Fig. 7. (Color online) Average spectral residuals between reconstructed and measured spectra on the Macbeth Color Checker DC test set

Appendix

In Tables 5-7 the results of the sensitivity analysis of the optimization function of Eq. (18) with respect to the various terms of which it is composed are reported. The analysis is simplified changing one weight at a time and assuming $\beta = \gamma$. Nine different values for each weight are considered: 0 (i.e. the corresponding term is not considered in the optimization), 0.001, 0.01, 0.1, 1, 10, 100, 1000, and setting all the other weights to 0 (i.e. the corresponding term is the only one considered in the optimization). The analysis results are reported in terms of average ΔE_{94} colorimetric error under the CIE D65 illuminant, and average GFC, for all the datasets considered. It is possible to notice that the colorimetric and spectral error are both needed in the optimization function of Eq. (18) (see the first and last columns of Table 5 and 7). The shape feasibility terms, given the two-step nature of the proposed algorithm, do not seem to have a deep impact on the final solution. When only the shape feasibility terms are used (last column of Table 6) the final solution is similar to the ones obtained by the adaPCA and PCAmuBa algorithms (see Table 2).

References

1. D. Dupont, "Study of the reconstruction of reflectance curves based on tristimulus values: comparison of methods of optimization," Color Research and Application, **27**(2), 88–99 (2002).
2. X. Zhang and H. Xu, "Reconstructing spectral reflectance by dividing spectral space and extending the principal components in principal component analysis," Journal of Optical Society of America A, **25**(2), 371–378 (2008).
3. A. Mansouri and T. Sliwa and J.Y. Hardeberg and Y. Voisin, "An adaptive-pca algorithm for reflectance estimation from color images," in *Proceedings of the 19th IEEE International Conference on Pattern Recognition* (IEEE, 2008), pp. 1–4.
4. R. Penrose, "A generalized inverse for matrices," in *Proceedings of the Cambridge Philosophical Society*, **51**, 406–413 (1955).
5. H.S. Fairman and M.H. Brill, "The principal components of reflectances," Color Research and Application **29**, 104–110 (2004).
6. T. Harifi and S.H. Amirshahi and F. Agahian, "Recovery of reflectance spectra from colorimetric data using principal component analysis embedded regression technique," Optical Review, **15**(6), 302–308 (2008).
7. J. Hernández-Andrés, J. Romero, "Colorimetric and spectroradiometric characteristics of narrow-field-of-view clear skylight in Granada, Spain," Journal of Optical Society of America A, **18**(2), 412–420, (2001).
8. C.J. Hawkyard, "Synthetic reflectance curves by additive mixing," Journal of Society of Dyers and Colourists **109**, 323–329 (1993).
9. S. Zuffi and S. Santini and R. Schettini, "From color sensor space to feasible reflectance spectra," IEEE Transactions on Signal Processing, **56**(2), 518–531 (2008).
10. P. Comon, "Independent component analysis, a new concept?," Signal Processing, **36**(3), 287–314 (1994).
11. A. Hyvärinen, J. Karhunen, E. Oja, *Independent component analysis* (John Wiley & Sons, 2001).
12. R.M. Lewis and V. Torczon, "Pattern search methods for linearly constrained minimization," SIAM Journal on Optimization, **10**, 917–941 (2000).
13. M.J. Vhrel and R. Gershon and L.S. Iwan, "Measurement and analysis of object reflectance spectra," Color Research and Application, **19**(1), 4–9 (1994).
14. J. Lehtonen and J. Parkkinen and T. Jaaskelainen and A. Kamshilin, "Principal component and sampling analysis of color spectra," Optical Review, **16**(2), 81–90 (2009).
15. F. Wilcoxon, "Individual comparisons by ranking methods," Biometrics, **1**, 80–83 (1945).

Table 5. Sensitivity analysis of the optimization function with respect to the colorimetric error term ΔE_{94}, i.e. the weight α

Dataset	$[0, 100, 100, 1]$		$[10^{-3}, 100, 100, 1]$		$[10^{-2}, 100, 100, 1]$		$[10^{-1}, 100, 100, 1]$		$[1, 100, 100, 1]$		$[10^{1}, 100, 100, 1]$		$[10^{2}, 100, 100, 1]$		$[10^{3}, 100, 100, 1]$		$[1, 0, 0, 0]$	
	ΔE_{94}	GFC	ΔE_{94}	GFC	ΔE_{94}	GFC	ΔE_{94}	GFC	ΔE_{94}	GFC	ΔE_{94}	GFC	ΔE_{94}	GFC	ΔE_{94}	GFC	ΔE_{94}	GFC
MUNStr	19.8029	0.9965	0.0181	0.9974	0.0000	0.9974	0.0000	0.9974	0.0000	0.9974	0.0000	0.9974	0.0000	0.9974	0.0000	0.9974	0.0000	0.9972
MUNSte	20.1850	0.9961	0.0106	0.9967	0.0000	0.9967	0.0000	0.9967	0.0000	0.9967	0.0000	0.9967	0.0000	0.9967	0.0000	0.9967	0.0000	0.9965
VHRELte	24.5944	0.9782	0.5200	0.9832	0.0000	0.9854	0.0000	0.9854	0.0000	0.9854	0.0000	0.9854	0.0000	0.9854	0.0000	0.9854	0.0000	0.9843
MCCte	23.0726	0.9933	0.3170	0.9943	0.0000	0.9947	0.0000	0.9947	0.0000	0.9947	0.0000	0.9947	0.0000	0.9947	0.0000	0.9947	0.0000	0.9954
MDCte	21.7940	0.9957	0.0745	0.9964	0.0073	0.9964	0.0000	0.9964	0.0000	0.9964	0.0000	0.9964	0.0000	0.9964	0.0000	0.9964	0.0000	0.9959

Table 6. Sensitivity analysis of the optimization function with respect to the shape feasibility terms, i.e. the weights $\beta = \gamma$

Dataset	$[1, 0, 0, 1]$		$[1, 10^{-3}, 10^{-3}, 1]$		$[1, 10^{-2}, 10^{-2}, 1]$		$[1, 10^{-1}, 10^{-1}, 1]$		$[1, 1, 1, 1]$		$[1, 10^{1}, 10^{1}, 1]$		$[1, 10^{2}, 10^{2}, 1]$		$[1, 10^{3}, 10^{3}, 1]$		$[0, 1, 1, 0]$	
	ΔE_{94}	GFC	ΔE_{94}	GFC	ΔE_{94}	GFC	ΔE_{94}	GFC	ΔE_{94}	GFC	ΔE_{94}	GFC	ΔE_{94}	GFC	ΔE_{94}	GFC	ΔE_{94}	GFC
MUNStr	0.0000	0.9974	0.0000	0.9974	0.0000	0.9974	0.0000	0.9974	0.0000	0.9974	0.0000	0.9974	0.0000	0.9974	0.0000	0.9974	0.0000	0.9972
MUNSte	0.0000	0.9967	0.0000	0.9967	0.0000	0.9967	0.0000	0.9967	0.0000	0.9967	0.0000	0.9967	0.0000	0.9967	0.0000	0.9967	0.0002	0.9967
VHRELte	0.0000	0.9851	0.0000	0.9851	0.0000	0.9852	0.0001	0.9854	0.0000	0.9854	0.0000	0.9854	0.0000	0.9854	0.0000	0.9854	0.0036	0.9851
MCCte	0.0000	0.9947	0.0000	0.9947	0.0000	0.9947	0.0000	0.9947	0.0000	0.9947	0.0000	0.9947	0.0000	0.9947	0.0000	0.9947	0.0000	0.9946
MDCte	0.0000	0.9964	0.0000	0.9964	0.0000	0.9964	0.0000	0.9964	0.0000	0.9964	0.0000	0.9964	0.0000	0.9964	0.0000	0.9964	0.0008	0.9962

Table 7. Sensitivity analysis of the optimization function with respect to the spectral error term GFC, i.e. the weight δ

Dataset	$[1, 100, 100, 0]$		$[1, 100, 100, 10^{-3}]$		$[1, 100, 100, 10^{-2}]$		$[1, 100, 100, 10^{-1}]$		$[1, 100, 100, 1]$		$[1, 100, 100, 10^{1}]$		$[1, 100, 100, 10^{2}]$		$[1, 100, 100, 10^{3}]$		$[0, 0, 0, 1]$	
	ΔE_{94}	GFC	ΔE_{94}	GFC	ΔE_{94}	GFC	ΔE_{94}	GFC	ΔE_{94}	GFC	ΔE_{94}	GFC	ΔE_{94}	GFC	ΔE_{94}	GFC	ΔE_{94}	GFC
MUNStr	0.0000	0.9972	0.0000	0.9974	0.0000	0.9974	0.0000	0.9974	0.0000	0.9974	0.0000	0.9974	0.0000	0.9974	0.0181	0.9974	22.0189	0.9964
MUNSte	0.0000	0.9965	0.0000	0.9967	0.0000	0.9967	0.0000	0.9967	0.0000	0.9967	0.0000	0.9967	0.0000	0.9967	0.0106	0.9967	21.5030	0.9960
VHRELte	0.0000	0.9844	0.0000	0.9854	0.0000	0.9854	0.0000	0.9854	0.0000	0.9854	0.0000	0.9854	0.0000	0.9854	0.4280	0.9845	24.6220	0.9763
MCCte	0.0000	0.9954	0.0000	0.9947	0.0000	0.9947	0.0000	0.9947	0.0000	0.9947	0.0000	0.9947	0.0000	0.9947	0.3170	0.9943	22.4140	0.9933
MDCte	0.0088	0.9959	0.0089	0.9964	0.0088	0.9964	0.0088	0.9964	0.0000	0.9964	0.0000	0.9964	0.0074	0.9964	0.0746	0.9964	20.7156	0.9958